DOI: 10. 19884/j. 1672-5220. 202404013

Recent Advances in Transition Metal-Based Catalysts for Electrocatalytic Nitrate Reduction Reaction

LUO Hongxia[1], CHEN Jun[2], YANG Jianping[1]*

1. State Key Laboratory for Modification of Chemical Fibers and Polymer Materials, College of Materials Science and Engineering, Donghua University, Shanghai 201620, China
2. ARC Centre of Excellence for Electromaterials Science, Intelligent Polymer Research Institute, Australian Institute of Innovative Materials, University of Wollongong, New South Wales, Wollongong 2522, Australia

Abstract: The accumulation of excessive nitrate in the atmosphere not only jeopardizes human health but also disrupts the balance of the nitrogen cycle in the ecosystem. Among various nitrate removal technologies, electrocatalytic nitrate reduction reaction (eNO_3RR) has been widely studied for its advantages of being eco-friendly, easy to operate, and controllable under environmental conditions with renewable energy as the driving force. Transition metal-based catalysts (TMCs) have been widely used in electrocatalysis due to their abundant reserves, low costs, easy-to-regulate electronic structure and considerable electrochemical activity. In addition, TMCs have been extensively studied in terms of the kinetics of the nitrate reduction reaction, the moderate adsorption energy of nitrogen-containing species and the active hydrogen supply capacity. Based on this, this review firstly discusses the mechanism as well as analyzes the two main reduction products (N_2 and NH_3) of eNO_3RR, and reveals the basic guidelines for the design of efficient nitrate catalysts from the perspective of the reaction mechanism. Secondly, this review mainly focuses on the recent advances in the direction of eNO_3RR with four types of TMCs, Fe, Co, Ni and Cu, and unveils the interfacial modulation strategies of Fe, Co, Ni and Cu catalysts for the activity, reaction pathway and stability. Finally, reasonable suggestions and opportunities are proposed for the challenges and future development of eNO_3RR. This review provides far-reaching implications for exploring cost-effective TMCs to replace high-cost noble metal catalysts (NMCs) for eNO_3RR.

Key words: electrocatalysis; nitrate reduction reaction; transition metal-based catalyst (TMC); reaction mechanism; nitrogen cycle

CLC number: X703; TQ426 **Document code:** A

Article ID: 1672-5220(2024)04-0333-16

Open Science Identity
(OSID)

0 Introduction

Atmospheric nitrogen is one of the most important components in the composition of the atmosphere, and it is closely related to human life and development. In the earth's environment, the three main cycles include the water cycle, the carbon cycle and the nitrogen cycle. Among them, the nitrogen cycle is an important basic cycle in the biosphere, as shown in Fig. 1, which mainly involves the synthesis of organic nitrogen, ammonification, nitrification, denitrification and nitrogen fixation in organisms[1-3]. However, in recent years, imbalances in the nitrogen cycle caused by human activities (including the discharge of industrial wastewater, the burning of fossil fuels, the intensive use of fertilizers in agriculture and the indiscriminate discharge of human domestic wastewater) have led to alarming increases in nitrate levels in underground water and surface water, which are seriously disrupting nitrogen cycling in ecosystems and thus may pose a serious threat to biological health[4-6]. Among the various nitrogen-containing pollutants, nitrate is a non-ligand forming oxygen anion with high mobility, high solubility and stable presence in water bodies[7]. Once the water with high concentrations of nitrate flows back into the drinking water of human life, nitrates are partially reduced to nitrites when ingested into the human body, which is extremely hazardous to human health. Specifically, nitrite combines with ferritin in the blood, causing the latter to be oxidized into hyperferritin, which loses the ability to transport oxygen, easily inducing diseases such as infantile methemoglobinemia and congenital heart defect syndrome[8]. Some studies have also found that high concentrations of nitrate in drinking water can lead to diabetes mellitus, high blood pressure and hyperthyroidism; nitrite combines with ammonia in the

---

Received date: 2024-04-24

Foundation items: National Natural Science Foundation of China (Nos. 52172291 and 52122312); "Dawn" Program of Shanghai Education Commission, China (No. 22SG31)

* Correspondence should be addressed to YANG Jianping, email: jianpingyang@dhu.edu.cn

Citation: LUO H X, CHEN J, YANG J P. Recent advances in transition metal-based catalysts for electrocatalytic nitrate reduction reaction [J]. *Journal of Donghua University (English Edition)*, 2024, 41(4): 333-348.

stomach to form nitrosamines or their compounds, which have carcinogenic effects[9]. Many researchers have realized that the efficient and rapid green removal of NO_3^- pollution in water is of great difficulty and challenge in the field of water pollution control at present. Common methods for nitrate removal in water include biological, physicochemical and chemical methods. Biological methods mainly use denitrifying bacteria in bioreactors to reduce nitrate to harmless nitrogen under anaerobic conditions. However, under natural conditions, biological denitrification is often slow because the growth of denitrifying microorganisms is susceptible to various environmental factors. In addition, although nitrate can be completely degraded, the addition of organic carbon sources, e. g., methanol, poses the risk of contaminating drinking water with microorganisms and organic matter, and the production of bio-sludge in the process makes biological methods non-competitive with physicochemical methods for the treatment of drinking water[10]. Current physicochemical methods including adsorption, ion exchange, reverse osmosis and electrodialysis are effective nitrate removal methods. However, there are certain shortcomings, such as the generation of concentrated nitrate water, resulting in the risk of the secondary pollution of wastewater discharges as well as the additional operations and energy costs caused by the secondary treatment[11]. The traditional chemical method is to directly reduce the nitrate in the water by adjusting the pH of the nitrogen-containing wastewater and introducing H_2. However, the use of H_2 has a great safety risk, and it is prone to explode if it is not stored properly[12]. The photocatalytic method is an environmentally friendly nitrate removal method, but its reduction efficiency is still relatively low and not easy to realize the large-scale application[13]. Therefore, efficient and environmentally friendly removal of nitrogen-containing pollutants from water bodies, as well as minimizing the operating costs, is a pressing issue in the field of nitrogen removal. Electrocatalytic nitrate reduction reaction (eNO_3RR) is an efficient and environmentally friendly removal technology that has emerged in recent years. It has the advantages of good environmental compatibility and no secondary pollution, low maintenance costs, being easy to remote control and automation, being able to convert renewable energy (such as solar energy, wind and tidal energy) to electricity at room temperature and normal pressure and being easy to realize the promotion of laboratory scale to large-scale applications to some degree[14]. Therefore, it shows great advantages and application potential in purifying nitrate-polluted water and guaranteeing the safety of water bodies. Electrocatalytic nitrate reduction is a multi-electron transfer and proton coupling process involving valence changes from −5 to +3, in which various nitrogen-containing intermediates are formed as well as the by-products from side reactions such as hydrogen evolution reaction (HER). Therefore, a large number of researchers have invested in the design of nitrate electrocatalysts with high activity, high selectivity and high stability, which mainly include noble metal catalysts, non-noble metal catalysts and non-metal catalysts[15]. Although researchers are committed to developing a variety of non-metallic nitrogen-doped carbon-based electrocatalysts, the existing nitrogen-doped carbon materials have uncontrollability in controlling the type, number and uniformity of doping atoms or defects, leading to controversy over the active site of non-metallic electrocatalysts. Therefore, compared with traditional noble metal catalysts, transition metal-based catalysts (TMCs) not only exhibit excellent catalytic activity, but also reduce the cost of catalyst preparation to a certain extent due to their abundant reserves on earth, making them a promising class of catalysts. Figure 2 counts the number of publications on TMCs (Fe, Co, Ni and Cu) applied to eNO_3RR over the past decades according to the database of the Web of Science. It is obvious that Fe, Co, Ni and Cu have been increasingly studied in the field of eNO_3RR in recent years.

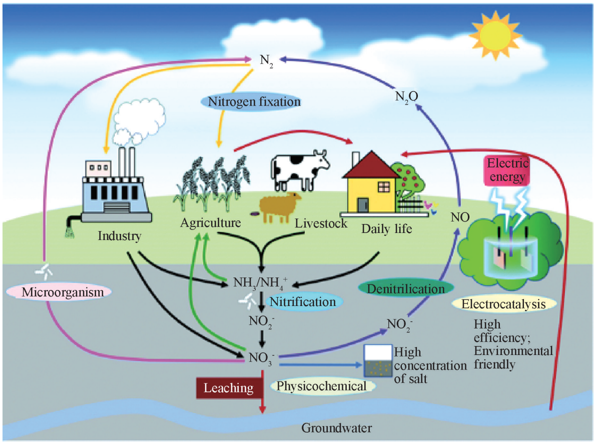

Fig. 1 Nitrogen cycle diagram in the ecosystem[3] (Copyright 2022, Royal Society of Chemistry)

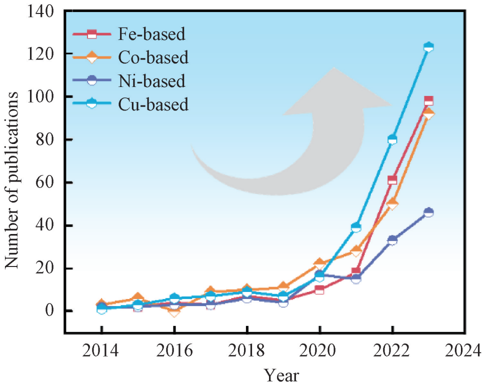

Fig. 2 Number of publications for TMCs (Fe, Co, Ni and Cu) over the past ten years (data is from the website Web of Science on April 4, 2024)

Therefore, this review summarizes the relevant research progress in the field of eNO_3RR by TMCs (Fe, Co, Ni and Cu) in recent years. Firstly, considering that the nitrate reduction process involves the transition of the valence state of nitrogen-containing species from +5 to −3, which makes the intermediates complex, this review analyzes and discusses the mechanism of eNO_3RR in depth. Then, the two most stable products of eNO_3RR, N_2 and NH_3, are categorized and discussed. Furthermore, the review highlights the recent advances of the transition metal-based electrocatalysts, including Fe, Co, Ni and Cu in the field of eNO_3RR to N_2 or NH_3. Finally, challenges and opportunities for future research and applications of eNO_3RR are discussed, aiming to provide a reference for the design and preparation of highly active and selective as well as highly stable TMCs for eNO_3RR.

1 Mechanism of eNO_3RR

For the time being, eNO_3RR can be divided into two main categories: indirect reduction and direct reduction. Indirect eNO_3RR is that NO_3^- itself does not participate in the electron transfer during the reduction reaction, but NO_3^- is first reduced to NO_2^- under high concentrations of nitrate as well as acidic conditions (Fig. 3(a)). The indirect catalytic reduction process is divided into two main pathways, namely Vetter and Schmid, both of which occur at low overpotentials.

The Vetter pathway involves a multiphase process, in which NO_2 is chemically regenerated at the catalytic interface. This process rarely relies on solution agitation because NO_2 production undergoes slow nonhomogeneous chemical reactions:

$$NO_2 + e^- \longrightarrow NO_2^-, \tag{1}$$

$$NO_2^- + H^+ \longrightarrow HNO_2, \tag{2}$$

$$HNO_2 + HNO_3 \longrightarrow N_2O_4 + H_2O, \tag{3}$$

$$N_2O_4 \longrightarrow 2NO_2. \tag{4}$$

In the Schmid pathway, a large amount of NO^+ electroactive species are produced, and the NO^+ is formed in layers close to the electrodes, so that the current decay is observed and the agitation has a strong influence on the process[16]. The chemical reactions are as follows.

$$HNO_2 + H^+ \longrightarrow NO^+ + H_2O, \tag{5}$$

$$NO^+ + e^- \longrightarrow NO, \tag{6}$$

$$HNO_3 + 2NO + H_2O \longrightarrow 3HNO_2, \tag{7}$$

$$N_2O_4 + 2NO + 2H_2O \longrightarrow 4HNO_2. \tag{8}$$

Direct eNO_3RR can be divided into the atomic hydrogen-mediated eNO_3RR and the electron-mediated eNO_3RR (Fig. 3(b))[17].

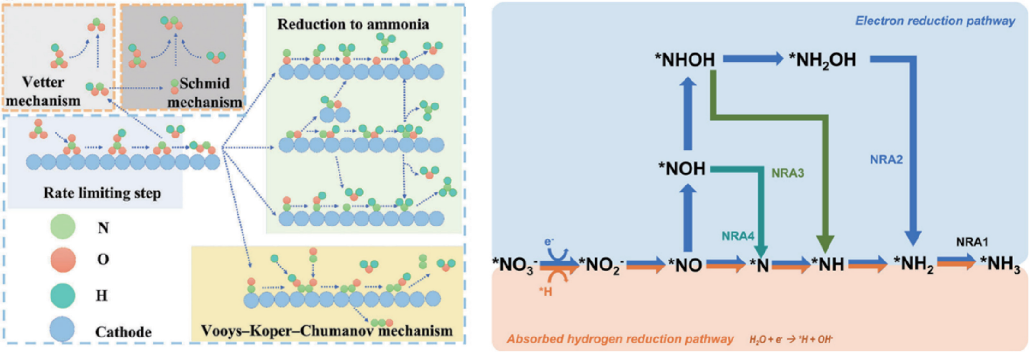

(a)

(b)

NRA—nitrate reduction to ammonia.

Fig. 3 Mechanism of eNO_3RR: (a) indirect reduction pathway for eNO_3RR in solution[16] (Copyright 2023, Wiley-VCH GmbH); (b) direct reduction pathway for eNO_3RR[17] (Copyright 2024, Royal Society of Chemistry)

The atomic hydrogen-mediated eNO_3RR begins with the reduction of H_2O adsorbed on the surface of the catalyst to product atomic hydrogen and hydroxide via a Volmer process, and then the atomic hydrogen adsorbed on the surface of the cathode progressively deoxygenates and hydrogenates the NO_2^- to produce NH_3 (Eqs. (9)–(19)). In short, for the formation of ammonia, the most direct reduction process is that NO_3^- is first deoxidized and then hydrogenated, and finally the reduction product NH_3 is obtained. The electron-mediated eNO_3RR begins with NO_3^- adsorbed on the surface of the catalyst, forming NO_3^- in the adsorbed state (NO_3(ads), ads denotes the adsorbed state). Then the NO_3(ads) is reduced to NO_2^- in the adsorbed state (NO_2(ads)) by the action of the electrons, and by this time, the NO_2(ads) may turn into NO_2^- in the free state, forming a product in very low concentration. This process is more difficult to occur and requires a higher energy barrier. Therefore, this process is usually considered as the rate-determining step of the eNO_3RR. Furthermore, NO_2(ads) is further reduced in the presence of electrons to produce NO intermediates (NO(ads)). It is worth mentioning that NO(ads) is a critical intermediate in the process of eNO_3RR, which can be adjusted by changing the type of electrolyte, the applied voltage and the pH of the electrolyte. They can determine the type of the product whether to produce N_2 or NH_3, etc. Therefore, this process is often referred to as the selectivity-determining step of the eNO_3RR. The eNO_3RR can take many paths to generate N_2. The most direct path is the removal of an oxygen atom from NO(ads) by the action of electrons to form an N intermediate (N(ads)), and then the combination of the two N (ads) to form N_2. The other major path (Eqs. (20)–(23)) to form N_2 is the combination of two NO(ads) to form N_2O (ads), which are electrically generated to form N_2. In Eq. (21), aq denotes aqueous solution state. In addition, ammonia produced by NO_3^- electroreduction in the electrolyte can be further oxidized to N_2 by electrochlorination (Eqs. (24)–(27)).

$$H_2O + e^- \longrightarrow H(ads) + OH^-, \quad (9)$$

$$NO_3^-(ads) + 2H(ads) \longrightarrow NO_2^-(ads) + H_2O, \quad (10)$$

$$NO_2^-(ads) + H(ads) \longrightarrow NO(ads) + OH^-, \quad (11)$$

$$NO(ads) + H(ads) + e^- \longrightarrow HNO(ads), \quad (12)$$

$$HNO(ads) + H(ads) + e^- \longrightarrow H_2NO(ads), \quad (13)$$

$$H_2NO(ads) + H(ads) + e^- \longrightarrow NH_2OH(ads), \quad (14)$$

$$NO(ads) + 2H(ads) \longrightarrow N(ads) + H_2O, \quad (15)$$

$$N(ads) + H(ads) \longrightarrow NH(ads), \quad (16)$$

$$NH(ads) + NH(ads) \longrightarrow N_2H_2, \quad (17)$$

$$NH(ads) + H(ads) \longrightarrow NH_2(ads), \quad (18)$$

$$NH_2(ads) + H(ads) \longrightarrow NH_3(ads), \quad (19)$$

$$N(ads) + N(ads) \longrightarrow N_2, \quad (20)$$

$$NO(ads) \longrightarrow NO(aq), \quad (21)$$

$$NO(ads) + NO(ads) + 2H^+ + 2e^- \longrightarrow N_2O(ads) + H_2O, \quad (22)$$

$$N_2O(ads) + 2H^+ + 2e^- \longrightarrow N_2 + H_2O, \quad (23)$$

$$2Cl^- \longrightarrow Cl_2 + 2e^-, \quad (24)$$

$$Cl_2 + H_2O \rightleftharpoons HClO + Cl^- + H^+, \quad (25)$$

$$HClO \rightleftharpoons ClO^- + H^+, \quad (26)$$

$$2NH_3 + 2ClO^- \longrightarrow N_2 + 2HCl + 2H_2O + 2e^-. \quad (27)$$

2 Classification of Products for eNO_3RR

The classification of the products for eNO_3RR is shown in Fig. 4. The products for eNO_3RR mainly have NH_3 and N_2 (Eqs. (28)–(29)). This is because these two products possess excellent thermodynamic stability, other nitrogen-containing products such as N_2O, NO, N_2H_2 and NH_2OH are not stable enough, and the proportion of these products are extremely low, so the content of these products can be negligible to some extent[18].

$$NO_3^- + 9H^+ + 8e^- \longrightarrow NH_3 + 3H_2O, \quad (28)$$

$$2NO_3^- + 12H^+ + 10e^- \longrightarrow N_2 + 6H_2O. \quad (29)$$

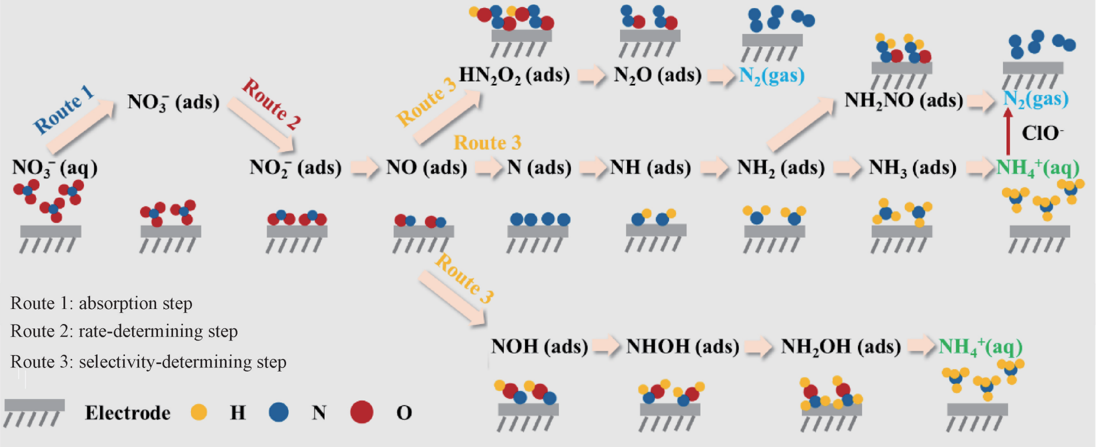

Fig. 4 Classification of products for eNO_3RR

2.1 Electrocatalytic nitrate reduction to NH_3

From an energy point of view, NH_3 is an irreplaceable chemical that has been widely demanded to keep modern societies sustainable, as a globally important industrial raw material (fertilizers, high-value chemicals and pharmaceuticals) and as a new-generation energy carrier. The conventional Haber-Bosch method for ammonia requires the breaking of the N≡N bond and the reaction with hydrogen to produce NH_3 at high temperatures (350 – 450 ℃) and high pressures (10–20 MPa)[19-20].

However, the high temperature and high-pressure conditions generate significant energy consumption. In addition, the H_2 required for the reaction process comes from the reaction of water vapor and methane at high temperatures and pressures. The CO produced during the process is converted to CO_2, which is harmful to the atmosphere[21]. Therefore, it is particularly important to find alternative methods of ammonia production. The high concentration of nitrogen-containing polluted wastewater is converted to ammonia under ambient conditions using renewable energy as the driving force through the method of electroreduction, which realizes zero emission while effectively removing nitrate pollutants in water, and significantly reduces the energy consumption required for the production and the cost of preparation, and therefore becomes a current research hotspot[22-24]. For example, Koper's group[25] systematically analyzed the potential applications of the electrocatalytic nitrate reduction process for ammonia synthesis. From the perspective of wastewater types, they pointed out the problems when nuclear wastewater, industrial wastewater and contaminated groundwater were used as sources of nitrate-containing wastewater for electrocatalytic reduction of ammonia, respectively, and proposed possible solutions and future research priorities. The feasibility of eNO_3RR for ammonia synthesis in terms of catalytic efficiency, energy consumption and economics was investigated through a comprehensive comparison with the industrial Haber-Bosch process. New ideas were provided for green ammonia synthesis by eNO_3RR from wastewater and balancing the global nitrogen cycle.

2.2 Electrocatalytic nitrate reduction to N_2

From the environmental point of view, the reduction of nitrate to non-toxic N_2 can effectively reduce the total nitrogen concentration in the water body without causing secondary pollution to the water body and the environment. In addition, according to the thermodynamic theory, N_2 exhibits the highest equilibrium potential among all the nitrate reduction products, so N_2 is the most stable product of nitrate reduction. In addition, for low-concentration nitrate wastewater (10 – 1 000 mg/L N), it would be more practical to convert it to N_2 rather than NH_3 by renewable electricity drive, mainly because it is extremely difficult to enrich NH_3 at low concentration, which obviously increases energy consumption[26]. For example, Zhao's group[27] employed two-dimensional phosphene as a ligand and anchored high-density PdCu diatoms on its surface to form a unique $PdCuP_4$ coordination structure, and applied it to nitrate reduction in water to achieve complete $N\equiv N$ bonding for nitrogen removal. Electrocatalytic nitrate reduction to N_2 for water purification should generally not introduce new contaminants, and the catalyst needs to be extremely stable to ensure no dissolution during nitrate removal. Therefore, it is very important to develop highly active and stable catalysts for eNO_3RR.

In summary, the process of eNO_3RR involving a variety of nitrogen-containing intermediates is extremely complex, and the reaction process is inevitably accompanied by the occurrence of competing HER. The structural design of catalysts is one of the key factors to determine the catalytic performance. It is considered to be one of the considerable strategies to rebalance the nitrogen cycle to explore the economical electrocatalysts for eNO_3RR to replace the high-cost noble-metal catalysts. In addition, it is necessary to use a variety of advanced in-situ characterization techniques to monitor the structural changes of the reaction catalysts as well as the nitrogen-containing intermediates in the reaction process in time[28]. This leads to a better understanding of the process of eNO_3RR, thus enabling targeted regulation of reaction pathways and the development of promising catalysts. In recent years, TMCs, especially Fe, Co, Ni and Cu, have shown great advantages in the field of eNO_3RR. TMCs not only have the advantages of controllable structural design, but also have performance comparable to that of noble metals. Therefore, TMCs have made a huge leap forward in the field of eNO_3RR.

3 TMCs for eNO_3RR

3.1 Fe-based catalysts

Metallic Fe is not only abundant on earth, but also plays an important role in the natural nitrogen cycle. Therefore, numerous researchers have invested in the study of Fe-based catalysts for eNO_3RR[29-31]. For example, in order to increase the metallic Fe content in the catalyst, Su et al.[32] prepared a corchorifolius-like iron-carbon composite (CL-Fe@C) with up to 74 % (mass fraction) Fe using a self-assembly method (Fig. 5(a)). The nitrate removal capacity of CL-Fe@C was as high as 1 816 mg (for 1 g Fe), with an N_2 selectivity of close to 100%[32]. In addition, to better expose the Fe active sites and improve the utilization of metallic Fe active sites, Zhang et al.[33] assembled carbon-coated Fe nanocrystals with one-dimensional carbon nanofibers by an interfacial assembly method. As shown in Fig. 5(b), the Fe nanoparticles were uniformly distributed on the fiber surface. The interaction between Fe nanoparticles and fiber supports resulted in nitrate removal of 2 317 mg (for 1 g Fe) as well as 97.2% N_2 selectivity[33]. In recent years, single-atom catalysts have been widely used in a variety of homogeneous or multiphase catalytic reactions due to their high specific surface area and high active site utilization, and have shown excellent catalytic activity and selectivity[34-36]. For example, Xu et al.[37] prepared a single atom Fe and a hybrid catalyst Fe_3C by high-temperature pyrolysis for eNO_3RR to ammonia. Among them, Fe single-atom was used as the main active site for eNO_3RR, while Fe_3C was used as the catalytic site for active hydrogen generation. The synergistic effect between Fe single-atoms and Fe_3C resulted in a Faraday efficiency of ammonia close to 100% and an even higher ammonia yield of 24 768 μg/(h · cm^2) at −0.4 V versus the reversible hydrogen electrode (vs. RHE) for eNO_3RR (Figs. 5(c) and 5(d))[37]. Since the eNO_3RR is a multi-electron and proton-coupled process and involves the adsorption and transformation of multiple nitrogen-containing intermediates, a single active site is not sufficient to enable rapid adsorption and transformation of intermediates, which results in low reactivity[38]. Therefore, our group employed in situ electrodeposition to dope Cu ions from the electrolyte into Fe-based catalysts (Cu-Fe/Fe_3C@NCNFs) loaded on the carbon nanofibers. This bimetallic synergism effectively enhanced the NO_3^- to NO_2^- conversion, which elevated the rate-determining step of eNO_3RR, and thus accelerated the reaction rate, achieving a nitrate removal capacity of 15 593.8 mg (for 1 g Fe) (Figs. 5(e) and 5(f))[39]. In addition, the strong interaction between the Fe-Cu diatomic catalyst could promote the adsorption and conversion of NO_3^- (Fig. 5(g)). This strong interaction originates from the *d* orbital interaction between Fe and Cu atoms, which effectively reduced the overall reaction energy barrier, promoted the splitting of N—O bonds, and improved the efficiency of eNO_3RR (Fig. 5(h))[40]. Besides, Fan's group[41] prepared an ultrathin nanosheet-assembled RuFe nanoflower electrocatalyst for electrocatalytic nitrate reduction to ammonia using a one-pot method. The results of experiments and theoretical calculations demonstrated that the introduction of low-coordinated Ru could enhance the electrochemical activity of the RuFe catalyst and effectively regulate the d-band center of the catalyst to ensure effective electron transfer, which led to the low-energy barriers for nitrate reduction[41]. It has always been one of the key scientific issues to enhance the activity while still maintaining the stability of the catalyst whether the technology of eNO_3RR can be applied industrially or not. Therefore, in order to solve the problems of thermal agglomeration of Fe-based catalysts during the synthesis process as well as easy oxidation and corrosion during the electrocatalytic process, our group has made some contributing research works in this field. By using graphene as the carbon support, Fe nanoparticles were effectively encapsulated in a monolayer of graphene by hydrothermal as well as high-temperature thermal reduction strategies. Compared with the uncoated Fe nanoparticles, on the one hand, the Fe nanoparticles coated by the graphene-chainmail inhibited the agglomeration during high-temperature thermal reduction and effectively exposed more Fe active sites; on the other hand, due to the protective effect of the graphene chainmail, it effectively prevented the oxidation of the Fe nanoparticles by the oxygen in the electrolyte and prevented the leakage of the Fe ions in the electrolyte during the eNO_3RR (Fig. 5(i))[42]. In addition, our group has also designed a rice-like nitrogen-doped carbon-coated Fe_2N electrocatalyst by nitriding strategy. This Fe-N interface was designed not only with excellent acid and alkali corrosion resistance as well as superior capability for the supplement for active hydrogen species, but also the nitrogen-doped carbon (NC) shell protected the internal Fe_2N and enhanced the intrinsic activity of the Fe-based catalysts with excellent long-term cycling stability: an impressive 90% nitrate removal retention rate was maintained even after 40 cycles. (Fig. 5(j))[43]. This strategy of catalyst stability regulation is not only applicable to the eNO_3RR, but also to other electrocatalytic reactions.

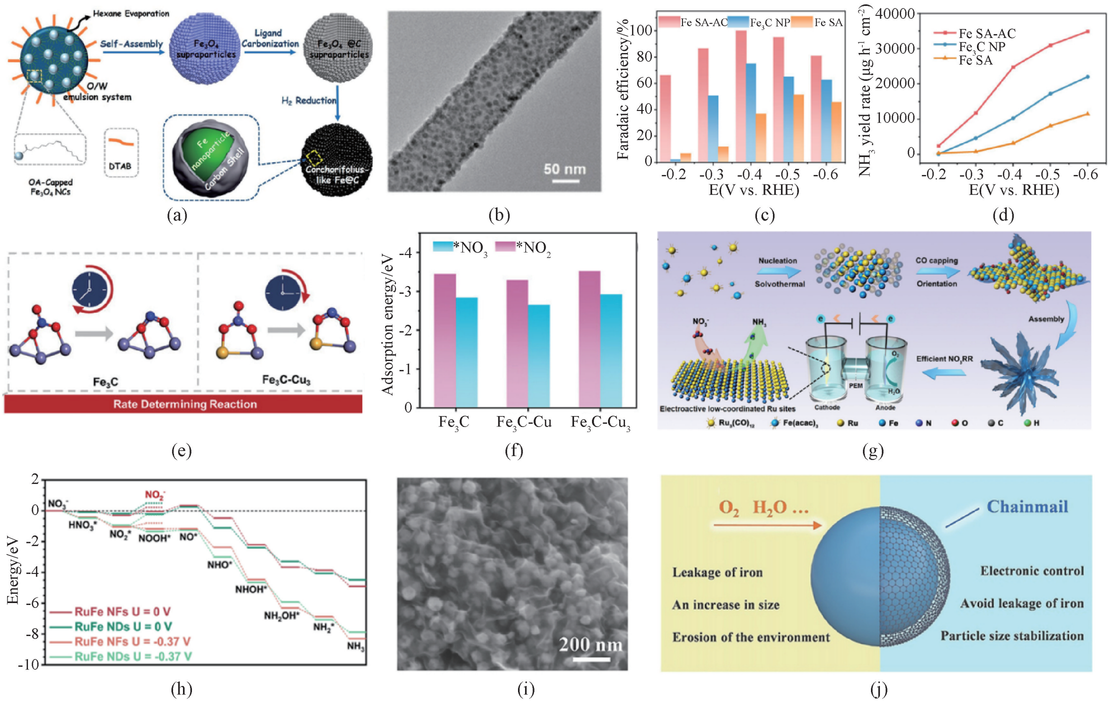

(a) (b) (c) (d)

(e) (f) (g)

(h) (i) (j)

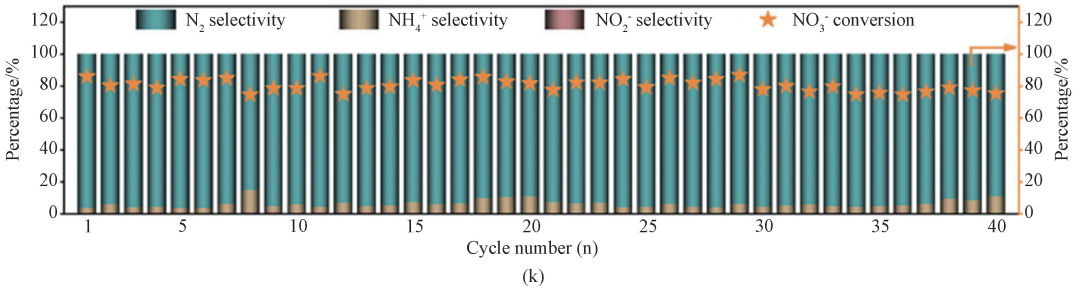

SA—single-atom; AC—active carbon; NP—nanoparticle; *—transition state.

Fig. 5 Fe-based catalysts for eNO_3RR: (a) schematic illustration of CL-Fe @ C[32] (Copyright 2019, American Chemical Society); (b) transmission electron microscopy (TEM) images of Fe_3O_4/NFs[33] (Copyright 2023, Wiley-VCH GmbH); (c)–(d) Faradaic efficiency and NH_3 yield rate[37] (Copyright 2024, American Chemical Society); (e) boosted effect of Cu sites on the transformation of $^*NO_3$ to $^*NO_2$[39] (Copyright 2024, Wiley-VCH GmbH); (f) absorption energy of $^*NO_3$ and $^*NO_2$ for Fe and Cu sites, respectively[39] (Copyright 2024, Wiley-VCH GmbH); (g) catalytic conversion pathways from nitrate to NH_3[40] (Copyright 2023, the authors, Springer Nature); (h) partial density of states of Fe/Cu 3d orbitals[40] (Copyright 2023, the authors, Springer Nature); (i) scanning electron microscopy (SEM) image of graphene-nanochainmail-protected iron nanoparticle (Fe@Gnc)[42] (Copyright 2022, Wiley-VCH GmbH); (j) roles of graphene nano-chainmail in eNO_3RR[42] (Copyright 2022, Wiley-VCH GmbH); (k) stability of the nitrogen-doped carbon-coated rice-like iron nitride (RL-Fe_2N@NC) for eNO_3RR[43] (Copyright 2023, Wiley-VCH GmbH)

3.2 Co-based catalysts

Co-based catalysts are a promising electrocatalyst for nitrate reduction because they exhibit good NO_3^- activation and hydrogenation for $^*N$ intermediate in the eNO_3RR process. Since the oxidized state of Co as well as the electron-rich metal Co are relatively poor for NO_3^- adsorption as well as NO_3^- to NH_3 activity, Yang et al.[44] designed an electron-deficient Co nanocrystal to facilitate the electrocatalytic NO_3^- reduction for the synthesis of NH_3 by Co interaction with pyridine nitrogen (Co/PN-C). Theoretical calculations showed that the pyridine nitrogen induced the formation of an electron-deficient structure of Co, which in turn enhanced the adsorption of NO_3^- as well as decreased the hydrogenation energy barrier from $^*NH$ to $^*NH_2$, enabling Co/PN-C to achieve an ammonia Faradaic efficiency as high as 97.2% and a NO_3^- removal rate close to 100% (Figs. 6(a) and 6(b))[44]. In order to enhance the supply capacity of active hydrogen during the nitrate reduction process, the electronic structure of the transition metal was modulated by introducing heteroatoms containing high electronegativity or creating more defective structures, so as to enable it not only to produce more active hydrogen, but also to provide a sufficient number of active hydrogen adsorption sites, and thus enhance the intrinsic activity of the catalyst[45-46]. An electron-rich Co site confined in the open backbone could rationally regulate the supply of active hydrogen as well as the N_2 product selectivity and reaction rate (Fig. 6(c))[47]. In addition, Lu's group prepared a three-dimensional network structure with Co-carbon nanofibers (Co-CNF) as the core and ZIF-67-derived amorphous CoP as the shell (Co-CNF/ZIF-CoP) for eNO_3RR. The amorphous CoP efficiently lowered the energy barrier associated with the critical rate-determining step, transforming $^*NO$ to $^*NOH$ during the reaction process. This facilitation enabled a remarkable 96.8% ammonia Faraday efficiency, alongside an ammonia yield of (38.44 ± 0.65) mg/(h · cm^2) within a potential range from −0.6 V to 0.1 V vs. RHE. (Figs. 6(d)–6(f))[48]. In addition to the ability to supply active hydrogen species, it is also important to introduce a second metal into the based electrocatalyst to modulate the electronic structure of Co as well as the regulation of the reaction pathway[49-51]. Chu's group[52] designed a single-atom CoRu alloy (Co_1Ru) as an efficient and durable catalyst. Thanks to the synergistic catalytic effect of the Co_1-Ru bimetallic alloy, the Co_1Ru catalyst exhibited excellent adsorption as well as hydrogenation of NO_2^- (Fig. 6(g)). In addition, Zhang's group[53] designed a Ru_xCo_y alloy catalyst model and proposed a three-step relay mechanism consisting of spontaneous redox reaction, electrochemical reduction, and electrocatalytic reduction to achieve efficient eNO_3RR to ammonia production at a low overpotential. In particular, the energy efficiency of $Ru_{15}Co_{85}$ at 0.4 V vs. RHE was up to (42 ± 2)% and the NH_3 generation rate could reach up to (3.20 ± 0.17) mol/h for 1 g catalyst, with a corresponding Faradaic efficiency of (97 ± 5)%. The results of theoretical calculations also indicated that the $Ru_{15}Co_{85}$ alloy was thermodynamically very favorable for N—O bond cleavage. Although Co-based electrocatalysts have achieved excellent performance, the reaction mechanism and the real active substance in a wide potential range are still controversial. Therefore, Yu's group[54] employed CoP, Co and Co_3O_4 as model materials to address these issues. Experimental results showed that CoP evolved into the core @ shell structure of CoP@Co prior to ammonia production from nitrate. For both CoP@Co and Co, a three-step relay mechanism was carried out on the surface dynamic $Co^{\delta+}$ active species at low overpotentials, whereas a sequential hydrogenation mechanism from nitrate to ammonia was revealed for the surface Co species at high overpotentials (Fig. 6(h)). In contrast, Co_3O_4 substances were stable and could stably catalyze the hydrogenation of nitrate to ammonia over a wide range of potentials. As a result, CoP@Co and Co exhibited much higher nitrate ammonia-producing activity than Co_3O_4, especially at low overpotentials (Fig. 6(i)). A series of characterizations elucidated the reason for the enhanced performance, emphasizing that the CoP nucleus provided abundant electrons to the surface-active species, resulting in the production of more active hydrogen for the reduction of nitrogenous intermediates (Fig. 6(j)).

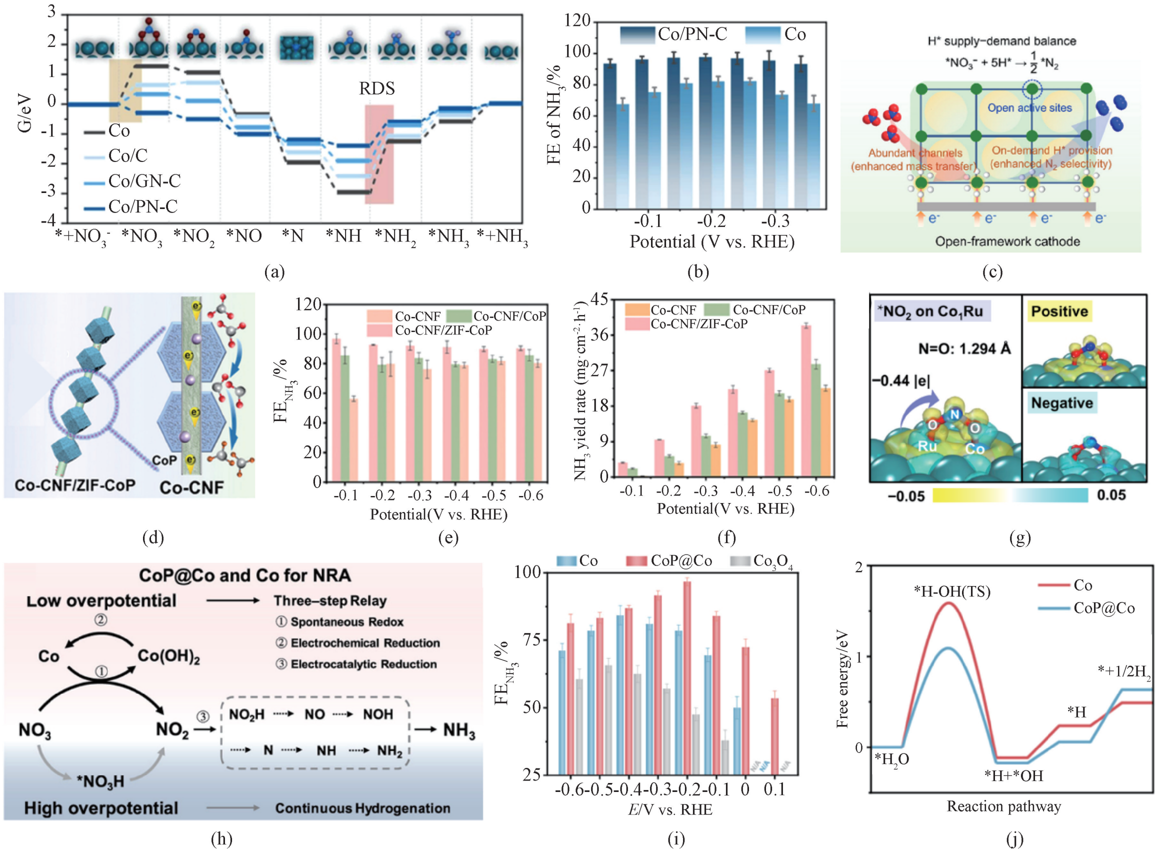

(a) (b) (c) (d) (e) (f) (g) (h) (i) (j)

Fig. 6 Co-based catalysts for eNO_3RR: (a) free energy diagram for each intermediates state on Co, Co/C, Co/GN-C and Co/PN-C[44] (Copyright 2023, Elsevier, all rights reserved); (b) performance of Co/PN-C under different potentials[44] (Copyright 2023, Elsevier, all rights reserved); (c) illustration of open-framework cathode for nitrate reduction to N_2 with the demand of $^*H$[47] (Copyright 2022, American Chemical Society); (d) preparation of Co-CNF/ZIF-CoP[48] (Copyright 2023, Wiley-VCH GmbH); (e)–(f) performances of Co-CNF, Co-CNF/CoP and Co-CNF/ZIF-CoP for the eNO_3RR[48] (Copyright 2023, Wiley-VCH GmbH); (g) charge density difference of $^*NO_2$ on Co_1Ru[52] (Copyright 2023, Tsinghua University Press); (h) diagram for CoP@Co and Co with a three-step relay mechanism and continuous hydrogenation mechanism[54] (Copyright 2024, American Chemical Society); (i) performance over CoP@Co, Co and Co_3O_4[54] (Copyright 2024, American Chemical Society); (j) Gibbs free energy of HER over CoP@Co and Co[54] (Copyright 2024, American Chemical Society)

3.3 Ni-based catalysts

It has been shown that HER in eNO_3RR is the largest competitive reaction, which seriously reduces the efficiency of nitrate reduction, so the researchers will choose the metal that is weaker for the HER reaction to be the catalytic activity center[55-57]. However, the active hydrogen required in the nitrate reduction process comes from water splitting. How to fully utilize the active hydrogen generated from HER to accelerate the reaction rate while also enhancing energy efficiency is another key scientific issue faced by the eNO_3RR. Numerous researches have shown that Ni-based catalysts have significant advantages in the HER process, which further indicates that Ni-based catalysts are favorable to the generation of active hydrogen, and to a certain extent, they can enhance the activity of ammonia production by nitrate reduction[58-60]. Structurally stable Ni metal-organic framework (Ni-MOF) nanosheets with large electrochemically active surface area and low electron transfer resistance were prepared by Pan et al.[61] through a one-step solvothermal method (Fig. 7(a)). Compared with the pure Ni foam support, the linear sweep voltammetry (LSV) curves showed that the Ni-MOF/NF exhibited superior performance for eNO_3RR in the electrolyte with 0.1 mol/L Na_2SO_4 and 1.5 g/L $NaNO_3$ (Fig. 7(b)). In addition, it was further verified by density functional theory (DFT) calculations that Ni atoms in the Ni(OH) microenvironment possessed superior

eNO_3RR performance than Ni atoms in the Ni (O) microenvironment. The conversion of adsorbed nitrate to adsorbed nitrite was considered as the rate-determining step of the nitrate reaction (Fig. 7(c)). The final catalyst exhibited 96.4% NO_3^- removal and a high ammonia yield of 110.13 μg/(h · cm^2)[61]. In addition, inspired by the biological enzymes in denitrifying bacteria, Hu et al.[62] designed a MOF-derived carbon-coated Ni phosphide (NiPC) catalyst for eNO_3RR to ammonia (Fig. 7(d)). The modulation of Ni valence could be achieved by adjusting the degree of phosphorylation, which further enhanced the hydrogenation activity of NO_3^-. The optimal NiPC catalyst achieved 96.88% ammonia Faraday efficiency at low nitrate concentration and near 100% selectivity to NH_3 (Fig. 7(e)). The diversity of eNO_3RR pathways makes it somewhat of a hindrance to product selectivity. Based on this, Ajmal and his co-authors designed a B and N co-doped graphene (BNG) as a support-loaded Ni monoatomic catalyst to achieve up to 168 μg/(h · cm^2) ammonia production activity as well as 98% ammonia Faraday efficiency (Fig. 7(f)). This excellent ammonia production activity was attributed to the ionic nature of the BNG support providing a redundant electric field effect that could enhance nitrate adsorption[63]. In addition, Gao's group proposed an electrical pulse-driven peroxidation and self-healing strategy for Ni-based catalysts modelled on Cu-Ni tandem catalysts. As shown in Figs. 7(g) and 7(h), the in-situ generation of highly active Cu/Cu_2O interface from Cu under pulse conditions breaks through the rate-limiting step of NO_3^- to NO_2^-. Meanwhile, the in situ conversion of Ni into $Ni/Ni(OH)_2$ interface and the modulation of hydrogen species adsorption promote the conversion of intermediates, which ultimately equilibrates NO_3^- to NO_2^- and NO_2^- to NH_3 reaction kinetics, realizing efficient electrocatalytic nitrate reduction for ammonia production[64].

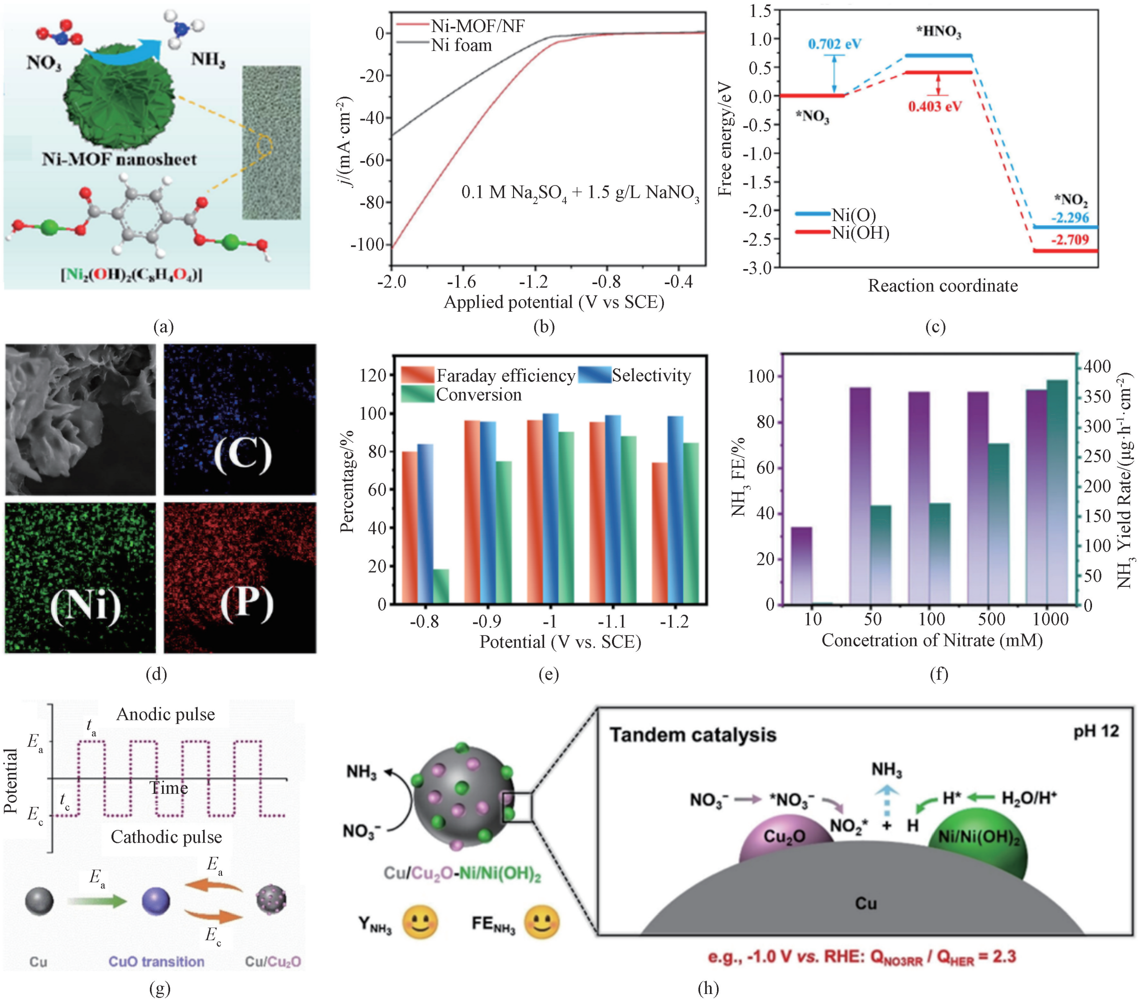

(a) (b) (c)

(d) (e) (f)

(g) (h)

0.1 M—0.1 mol/L.

Fig. 7 Ni-based catalysts for eNO_3RR: (a) schematic illustration for the synthesis route of Ni-MOF nanosheets[61] (Copyright 2023, Elsevier, all rights reserved); (b) LSV curves of Ni-MOF/NF and Ni foam (Copyright 2023, Elsevier, all rights reserved)[61]; (c) Gibbs free energy diagrams on Ni(OH) and Ni(O) sites of Ni-MOF for the $^*NO_3^-$ to $^*NO_2$ reaction[61] (Copyright 2023, Elsevier, all rights reserved); (d) elements mapping images for NiPC-1[62] (Copyright 2024, Tsinghua University Press); (e) performance of NiPC-1 catalyst[62] (Copyright 2024, Tsinghua University Press); (f) performance of NiSA@BNG catalyst[63] (Copyright 2024, Wiley-VCH GmbH); (g) pulsed electrolysis and changes of Cu valence state under pulse reaction conditions[64] (Copyright 2023, Wiley-VCH GmbH); (h) Tandem reaction schematic illustration for $Cu_{50}Ni_{50}$ under pulsed NO_3RR[64] (Copyright 2023, Wiley-VCH GmbH)

3.4 Cu-based catalysts

In eNO_3RR systems, Cu-based catalysts have excellent thermodynamic and kinetic activity due to the lowest limiting potential and the fastest rate-determining step. The d orbitals of Cu-based catalysts are very similar to the lowest unoccupied p orbitals in NO_3^-. This unique property facilitates accelerated electron transfer, which lowers the limiting potential and speeds up the rate-determining step[65]. Nevertheless, the use of Cu-based catalysts for eNO_3RR has certain problems, such as surface passivation caused by long-term electrolytic conditions, ionic leakage, and accumulation of NO_2^- which poses a more serious hazard to water bodies[66]. In view of this, Yu's group[67] proposed a pulsed electrolysis strategy with a Cu single-atom gel (Cu SAG) electrocatalyst that not only enhanced the kinetics of the eNO_3RR, but also facilitated the cascade catalytic accumulation of NO_2^- species, thus increasing the Faraday efficiency and yield of ammonia (Fig. 8(a)). In addition, Wu's group[68] synthesized a Cu-based electrocatalyst with low-coordinated Cu atoms (Cu-LC), which exhibited a high NH_3 selectivity of up to 97.01% and an NH_3 production rate of 0.624 mmol/(h · cm^2) (Fig. 8(b)). Thanks to the introduction of low-coordinated Cu sites to bring the d-band center of Cu closer to the Fermi energy level, the adsorption of key intermediates $^*NO_2$ and $^*NO$ was enhanced, and the generation and hydrogenation processes of $^*NO_2$ were also effectively regulated to inhibit NO_2^- accumulation on the surface of Cu-LC, and a high ammonia selectivity was achieved (Fig. 8(c)). In addition to the above methods, the synergistic catalytic effect of bimetallics can also effectively catalyze the reduction of a variety of nitrogen-containing intermediates and thus enhance the efficiency of the eNO_3RR. Sun's group[69] prepared a Cu@Ni Janus nanostructure, compared to the CuNi solid-solution alloy (SSA), the short-range ordered interfacial structure in this Janus structure effectively promoted the activation of NO, and the Ni-rich phase facilitated the H_2O cleavage to generate active hydrogen, and then $^*H$ spontaneously migrated to the neighboring catalytic sites to hydrogenate the $^*NO_x$ intermediates (Fig. 8(d)). Attributed to the synergistic effect of Cu and Ni bimetals, the catalyst possessed an ammonia yield of 1127 mmol/h with 1 g catlyst and a Faraday efficiency of 92.5% at −0.2 V vs. RHE (Fig. 8(e))[69]. The introduction of Se vacancies as well as doped heteroatoms can effectively modulate the electronic structure of Cu, which in turn accelerates the cleavage of $^*NO_3$ and stabilizes the $^*NO_2$ intermediate state, thus effectively improving the intrinsic eNO_3RR catalytic activity of Cu-based catalysts[70]. The noble metal Pd as a selectivity-determining radical in eNO_3RR is beneficial to enhance the selectivity of N_2, and when combined with Cu it can increase the rate-determining step[71-72]. In addition, the CuPd alloy exhibits excellent nitrate reduction activity and N_2 selectivity over the full pH range[73]. A mesoporous carbon nanotube domain-limited CuPd alloy nanoparticle was prepared as an electrocatalyst for nitrate reduction to N_2 by Xu et al.[74]. It exhibited close to 100% NO_3^- removal and 98% N_2 selectivity (Fig. 8(f))[74]. In addition to the problem of Cu-based catalysts for NO_2^- accumulation on the Cu-based catalysts, the stability regulation of Cu-based catalysts also needs to be considered[75]. Metal-support interactions not only modulate the electronic structure of the catalyst, but also act as a confinement effect on the metal active site, improving the long-term stability of the catalysts[76-77]. By loading Cu atoms onto a long-range disordered arrangement of amorphous CeO_x, it was not only capable of generating a large number of defect sites to effectively modulate the electronic structure of Cu, but also enhanced the proton hydrogen supplying ability of Cu-based catalysts, suppressed the competing HER, and improved the catalyst energy efficiency (Fig. 8(g))[78]. Among them, in situ tests showed that the active center of the eNO_3RR was monomeric Cu rather than Cu_2O, and DFT calculations further indicated that the amorphous CeO_x modulated the electronic structure of Cu, greatly facilitated the hydrolysis process, and successfully achieved a balance between the production and consumption of active hydrogen (Fig. 8(h)). Although the abundance of catalytically active sites on the surface of Cu-based catalysts makes them exhibit great advantages for eNO_3RR to synthesize ammonia, the low atom economy limits their large-scale application. Li's group[79] designed a high-atom-economy Cu single-atom doped into nitrogen-doped carbon electrocatalyst (Cu SA/NC). In comparison with the electrocatalysts with a mixture of Cu single-atom and Cu nanoparticles, Cu SA/NC exhibited an ammonia production efficiency close to 100% and an NH_3 yield of 7480 μg/h with 1 mg catalyst, and it effectively hindered the N—N coupling process and enhanced the energy efficiency of NH_3 (Fig. 8(i))[79].

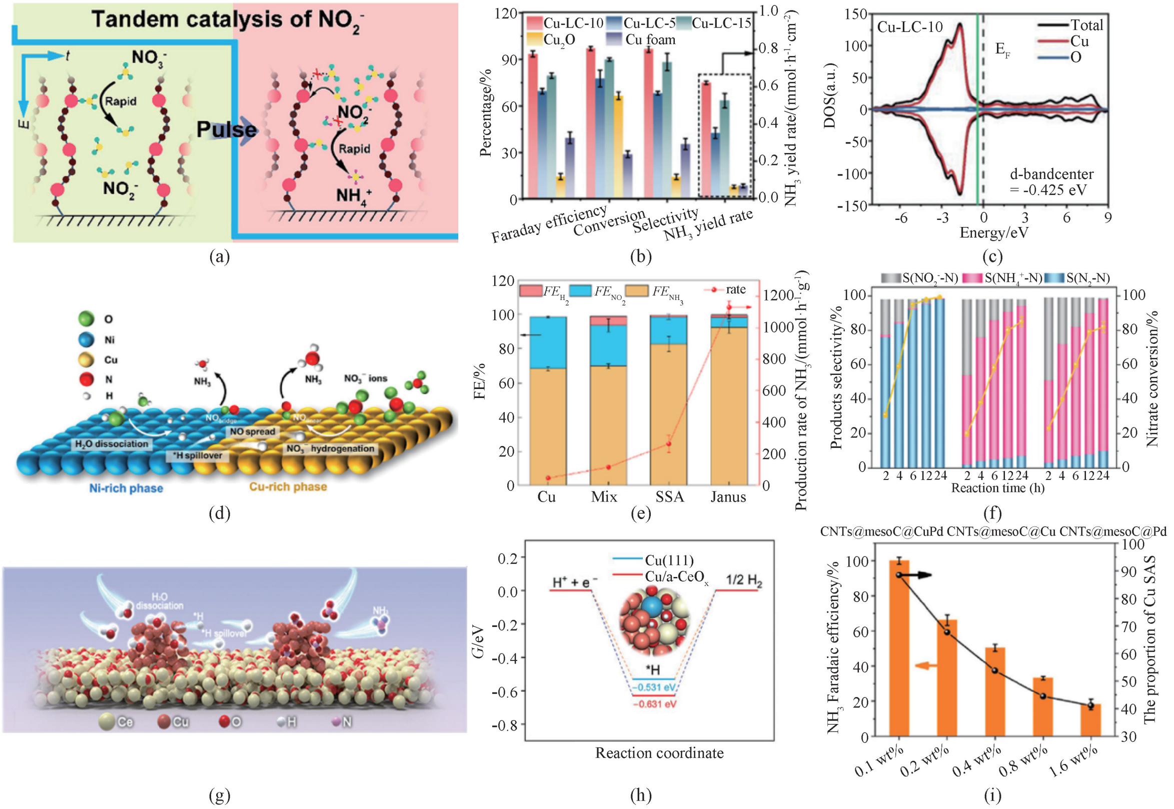

Fig. 8 Cu-based catalysts for eNO_3RR: (a) schematic illustration of the mechanism for eNO_3RR over Cu SAGs[67] (Copyright 2023, American Chemical Society); (b) performance for different samples at −0.8 V vs. RHE[68] (Copyright 2024, Wiley-VCH GmbH); (c) density of states (DOS) diagram of Cu-LC-10[68] (Copyright 2024, Wiley-VCH GmbH); (d) schematic illustration of the mechanism for the enhanced eNO_3RR over $Cu_{50}Ni_{50}$-Janus/C[69] (Copyright 2024, the authors, published by American Chemical Society); (e) performance over $Cu_{50}Ni_{50}$-Janus/C, $Cu_{50}Ni_{50}$-SSA/C-, $Cu_{50}Ni_{50}$-Mix/C-, Cu/C- and Ni/C-coated carbon cloth[69] (Copyright 2024, the authors, published by American Chemical Society); (f) performance of carbon nanotubes @ mesoporous carbon @ CuPd (CNTs@mesoC@CuPd), CNTs@mesoC@Cu and CNTs@mesoC@Pd at different reaction time for eNO_3RR[74] (Copyright 2022, Wiley-VCH GmbH); (g) schematic illustration of the mechanism for Cu/a-CeO_x catalyzed eNO_3RR[78] (Copyright 2023, Wiley-VCH GmbH); (h) DFT calculation of eNO_3RR and HER on Cu (111) and Cu/a-CeO_x[78] (Copyright 2023, Wiley-VCH GmbH); (i) Faraday efficiencies of NH_3 for different proportions of Cu SAs in Cu SA/NC and Cu_{s+n}/NC[79] (Copyright 2023, American Chemical Society)

In conclusion, TMCs play a significant role in eNO_3RR. For the regulation of catalytic activity, heteroatom doping and bimetallic synergism can effectively regulate the electronic structure of transition metals, and then regulate the d-band center to optimize the adsorption/desorption conversion of intermediate states and enhance the nitrate reduction activity. For the optimization of the reaction pathway, the adsorption conversion of the intermediates in the eNO_3RR and the control of the local microenvironment can be regulated through the construction of multi-metal sites or heterogeneous interfaces to realize an effective tandem catalytic mechanism. For the improvement of catalyst stability, metal-support interactions as well as nano-confined engineering strategies and nano-chainmail protection can effectively protect transition metal catalysts from easy oxidation and high-temperature thermal agglomeration, which can fully expose more effective catalytic active sites. Furthermore, the transition metal single-atom catalysts can enhance the atom utilization and increase the catalytic activity. In addition to the above summary of eNO_3RR, the design strategies of TMCs, such as crystal surface engineering, defect engineering, built-in electric field construction and alloying, have also been reasonably considered.

4 Summary and Outlook

Electrocatalytic nitrate reduction is a green and highly efficient nitrate removal technology, especially showing great advantages in NH_3 synthesis compared with Haber-Bosch process. In this review, the mechanism of eNO_3RR is discussed in depth as well as the two stabilized products (N_2 and NH_3) are analyzed separately from the perspectives of environment and energy. Then, the following key issues are proposed for the design of efficient catalysts for eNO_3RR.

1) Regarding adsorption of NO_3^- by the catalysts and the key step of NO_3^- to NO_2^- conversion, suitable metal site exposure and microenvironmental control at the electrode-electrolyte interface can effectively enhance the adsorption and conversion of NO_3^-.

2) For the selectivity of nitrate reduction products, a high concentration of nitrate wastewater is more favorable to the formation of NH_3, while a low concentration of nitrogen-containing wastewater is favorable to the formation of N_2. The durability of the catalyst in the actual nitrogenous wastewater treatment process needs to be reasonably solved.

3) The main cathodic competition HER during the reaction process can decrease the energy efficiency of eNO_3RR, and the active hydrogen species produced by the HER process of TMCs are reasonably utilized to inhibit the HER and enhance the energy efficiency.

Although the eNO_3RR has made great progress in performance and catalyst design, the following key issues need to be solved to achieve further development.

1) Although numerous catalysts have already demonstrated high Faraday efficiency and yields for the synthesis of NH_3 through nitrate reduction, the issue of collecting NH_3 from aqueous solutions and its subsequent utilization has not been adequately addressed in many research works. C—N coupling of NO_3^- reduction reaction with CO_2 or organic small molecules such as oxalic acid and methanol to prepare more valuable products is also necessary[80]. In particular, the synthesis of urea with CO_2 and NO_3^- has attracted academic interest, which can help reduce the carbon footprint while repairing nitrate-contaminated water caused by industrial emissions or improper release of agricultural fertilizers.

2) For the study of the electrocatalytic nitrate mechanism, in addition to the advanced in situ characterization techniques to detect the nitrogenous species converted by NO_3^- during the reaction process and then to analyze the reaction pathway, the influence of the catalyst rearrangement phenomenon on the reaction mechanism due to the influence of the electrolyte and the voltage during the reaction process also needs to be fully considered. For example, in-situ X-ray diffraction (XRD), in-situ Raman, in-situ Fourier transform infrared spectroscopy (FTIR) and in situ X-ray absorption near edge structure (XANES) are used to monitor the structural evolution of the catalysts during eNO_3RR.

3) To screen suitable materials for electrocatalytic nitrate catalysts more efficiently and quickly, and to reduce unnecessary resource consumption, machine learning can pre-construct a reasonable catalyst model, quickly screen efficient nitrate electrocatalysts as well as select suitable catalysts for specific product selectivity control.

4) Most of the current nitrate reduction electrocatalysts are operated at higher constant potentials or constant currents, which not only generate huge power consumption but also increase the occurrence of competing HER. The search for lower energy consumption catalysts or the use of plasma discharges or pulses strategies can be effective in enhancing energy efficiency. In addition, the current eNO_3RR is more focused on the structural design of the catalysts, however, the actual application needs to be considered from the perspective of economic cost, so the subsequent eNO_3RR process should be as far as possible from the economic perspective to analyze the practicality of catalyst materials and energy consumption.

5) Although many nitrate reduction catalysts with fast reaction rates and good stability have been designed, more of them are still on the laboratory scale, and the modulation of catalyst activity as well as durability testing for pilot and larger scale electrocatalytic NO_3^- removal are rarely studied. The rational design and optimization of the reactors are also indispensable for the large-scale application of eNO_3RR. In addition, at present, electrocatalytic nitrate reduction is mostly carried out under neutral or alkaline conditions, however, with the rapid development of industry and agriculture, nitrate pollutants also exist in strongly acidic wastewater. Therefore, the catalysts under development should ideally be adaptable to the full pH range, thereby maximizing their applicability in the removal of diverse nitrogen-containing wastewaters.

References

[1] LEHNERT N, MUSSELMAN B W, SEEFELDT L C. Grand challenges in the nitrogen cycle[J]. *Chemical Society Reviews*, 2021, 50(6): 3640-3646.

[2] NAZEMI M, EL-SAYED M A. Managing the nitrogen cycle via plasmonic (photo) electrocatalysis: toward circular economy[J]. *Accounts of Chemical Research*, 2021, 54(23): 4294-4304.

[3] XU H, MA Y Y, CHEN J, et al. Electrocatalytic reduction of nitrate: a step towards a sustainable nitrogen cycle[J]. *Chemical Society Reviews*, 2022, 51(7): 2710-2758.

[4] ABASCAL E, GÓ MEZ-COMA L, ORTIZ I, et al. Global diagnosis of nitrate pollution in groundwater and review of removal technologies [J]. *Science of the Total Environment*, 2022, 810: 152233.

[5] TEMKIN A, EVANS S, MANIDIS T, et al. Exposure-based assessment and economic valuation of adverse birth outcomes and cancer risk due to nitrate in United States drinking water [J]. *Environmental Research*, 2019, 176:

108442.

[6] GU L, KUANG M, CHEN J, et al. Perspective of nitrate reduction and nitrogen neutral cycle [J]. *Chinese Journal of Structural Chemistry*, 2023, 42(6): 100067.

[7] WU Z Y, SONG Y H, LIU Y B, et al. Electrocatalytic nitrate reduction: selectivity at the crossroads between ammonia and nitrogen [J]. *Chem Catalysis*, 2023, 3(11): 100786.

[8] GRANT S B, AZIZIAN M, COOK P, et al. Factoring stream turbulence into global assessments of nitrogen pollution [J]. *Science*, 2018, 359(6381): 1266-1269.

[9] GU B J, ZHANG X M, LAM S K, et al. Cost-effective mitigation of nitrogen pollution from global croplands [J]. *Nature*, 2023, 613 (7942): 77-84.

[10] BAI Y, WANG S, ZHUSSUPBEKOVA A, et al. High-rate iron sulfide and sulfur-coupled autotrophic denitrification system: nutrients removal performance and microbial characterization [J]. *Water Research*, 2023, 231: 119619.

[11] TONG S, ZHANG S X, ZHAO Y, et al. Hybrid zeolite-based ion-exchange and sulfur oxidizing denitrification for advanced slaughterhouse wastewater treatment [J]. *Journal of Environmental Sciences*, 2022, 113: 219-230.

[12] SHI J L, GAO Y, ZANG L, et al. Performance of Pd/Sn catalysts supported by chelating resin prestoring reductant for nitrate reduction in actual water[J]. *Environmental Research*, 2021, 201: 111577.

[13] HOU Z A, CHU J F, LIU C, et al. High efficient photocatalytic reduction of nitrate to N_2 by core-shell Ag/SiO_2 @ cTiO_2 with synergistic effect of light scattering and surface plasmon resonance [J]. *Chemical Engineering Journal*, 2021, 415: 128863.

[14] ZOU X Y, CHEN C J, WANG C H, et al. Combining electrochemical nitrate reduction and anammox for treatment of nitrate-rich wastewater: a short review [J]. *Science of the Total Environment*, 2021, 800: 149645.

[15] WU Z Y, SONG Y H, GUO H C, et al. Tandem catalysis in electrocatalytic nitrate reduction: unlocking efficiency and mechanism [J]. *Interdisciplinary Materials*, 2024, 3(2): 245-269.

[16] LIU D, QIAO L L, PENG S Y, et al. Recent advances in electrocatalysts for efficient nitrate reduction to ammonia [J]. *Advanced Functional Materials*, 2023, 33(43): 2303480.

[17] ZHANG K E, LIU Y, PAN Z F, et al. Cu-based catalysts for electrocatalytic nitrate reduction to ammonia: fundamentals and recent advances [J]. *EES Catalysis*, 2024, 2(3): 727-752.

[18] FU X B. Some thoughts about the electrochemical nitrate reduction reaction [J]. *Chinese Journal of Catalysis*, 2023, 53: 8-12.

[19] VAN DER HAM C J M, KOPER M T M, HETTERSCHEID D G H. Challenges in reduction of dinitrogen by proton and electron transfer[J]. *Chemical Society Reviews*, 2014, 43 (15): 5183-5191.

[20] ZHANG K, CAO A, WANDALL L H, et al. Spin-mediated promotion of Co catalysts for ammonia synthesis [J]. *Science*, 2024, 383 (6689): 1357-1363.

[21] FENG A L, HU Y D, YANG X X, et al. ZnO nanowire arrays decorated with Cu nanoparticles for high-efficiency nitrate to ammonia conversion [J]. *ACS Catalysis*, 2024, 14(8): 5911-5923.

[22] HU Q, ZHOU W L, QI S, et al. Pulsed co-electrolysis of carbon dioxide and nitrate for sustainable urea synthesis [J]. *Nature Sustainability*, 2024, 7: 442-451.

[23] ZHAO Y L, DING Y X, LI W L, et al. Efficient urea electrosynthesis from carbon dioxide and nitrate via alternating Cu-W bimetallic C-N coupling sites [J]. *Nature Communications*, 2023, 14(1): 4491.

[24] LI Y, ZHENG S S, LIU H, et al. Sequential co-reduction of nitrate and carbon dioxide enables selective urea electrosynthesis [J]. *Nature Communications*, 2024, 15(1): 176.

[25] VAN LANGEVELDE P H, KATSOUNAROS I, KOPER M T M. Electrocatalytic nitrate reduction for sustainable ammonia production [J]. *Joule*, 2021, 5(2): 290-294.

[26] BAI L C, FRANCO F, TIMOSHENKO J, et al. Electrocatalytic nitrate and nitrite reduction toward ammonia using Cu_2O nanocubes: active species and reaction mechanisms [J]. *Journal of the American Chemical Society*, 2024, 146(14): 9665-9678.

[27] SUN J, YANG H X, GAO W Q, et al. Diatomic Pd-Cu metal-phosphorus sites for complete $N\equiv N$ bond formation in photoelectrochemical nitrate reduction [J]. *Angewandte Chemie International Edition*, 2022, 61(45): e202211373.

[28] FU C H, SUN J L, DU Y Y, et al. In-situ characterization technologies for electrocatalytic reduction nitrate to ammonia on copper-based catalysts [J]. *ChemCatChem*, 2024: e202301545.

[29] LIU Y J, CHENG R Y, REN H X, et al. Ultrasmall iron nanoparticle-decorated carbon black for high-efficiency nitrate-to-ammonia electrosynthesis and zinc-nitrate batteries [J]. *ACS Sustainable Chemistry & Engineering*, 2024, 12(9): 3780-3789.

[30] LAN Y, CHEN J L, ZHANG H, et al. Fe/Fe_3C nanoparticle-decorated N-doped carbon nanofibers

for improving the nitrogen selectivity of electrocatalytic nitrate reduction[J]. *Journal of Materials Chemistry A*, 2020, 8(31): 15853-15863.

[31] LUO H X, WANG C Q, CONG Y T, et al. Confinement engineering for enhanced electrocatalytic nitrate reduction by integrating B-doped graphene with iron catalysts for long-term stability [J]. *Inorganic Chemistry Frontiers*, 2023, 10(19): 5611-5621.

[32] SU L, HAN D D, ZHU G J, et al. Tailoring the assembly of iron nanoparticles in carbon microspheres toward high-performance electrocatalytic denitrification[J]. *Nano Letters*, 2019, 19(8): 5423-5430.

[33] ZHANG F Z, LUO J M, CHEN J L, et al. Interfacial assembly of nanocrystals on nanofibers with strong interaction for electrocatalytic nitrate reduction[J]. *Angewandte Chemie International Edition*, 2023, 62(38): e2310383.

[34] YU Y T, ZHU Z J, HUANG H W. Surface engineered single-atom systems for energy conversion[J]. *Advanced Materials*, 2024, 36(16): 2311148.

[35] GLOAG L, SOMERVILLE S V, GOODING J J, et al. Co-catalytic metal-support interactions in single-atom electrocatalysts[J]. *Nature Reviews Materials*, 2024, 9: 173-189.

[36] ZENG Y C, LI C Z, LI B Y, et al. Tuning the thermal activation atmosphere breaks the activity-stability trade-off of Fe-N-C oxygen reduction fuel cell catalysts[J]. *Nature Catalysis*, 2023, 6: 1215-1227.

[37] XU L, LIU T, LIU D, et al. Boosting electrocatalytic ammonia synthesis via synergistic effect of iron-based single atoms and clusters[J]. *Nano Letters*, 2024, 24(4): 1197-1204.

[38] LUO H X, WANG C Q, WANG J Q, et al. A strong metal-support interaction strategy for enhanced binder-free electrocatalytic nitrate reduction[J]. *Inorganic Chemistry Frontiers*, 2023, 10(15): 4526-4533.

[39] HUA Y L, SONG N, WU Z Y, et al. Cu-Fe synergistic active sites boost kinetics of electrochemical nitrate reduction[J]. *Advanced Functional Materials*, 2024: 2314461.

[40] ZHANG S, WU J H, ZHENG M T, et al. Fe/Cu diatomic catalysts for electrochemical nitrate reduction to ammonia [J]. *Nature Communications*, 2023, 14(1): 3634.

[41] WANG Y H, SUN M Z, ZHOU J W, et al. Atomic coordination environment engineering of bimetallic alloy nanostructures for efficient ammonia electrosynthesis from nitrate [J]. *Proceedings of the National Academy of Sciences of the United States of America*, 2023, 120(32): e2306461120.

[42] ZHANG H, WANG C Q, LUO H X, et al. Iron nanoparticles protected by chainmail-structured graphene for durable electrocatalytic nitrate reduction to nitrogen[J]. *Angewandte Chemie International Edition*, 2023, 62(5): e2217071.

[43] LUO H X, LI S J, WU Z Y, et al. Modulating the active hydrogen adsorption on Fe-N interface for boosted electrocatalytic nitrate reduction with ultra-long stability [J]. *Advanced Materials*, 2023, 35(46): 2304695.

[44] YANG B P, ZHOU Y L, HUANG Z C, et al. Electron-deficient cobalt nanocrystals for promoted nitrate electrocatalytic reduction to synthesize ammonia[J]. *Nano Energy*, 2023, 117: 108901.

[45] LU X M, YU J K, CAI J M, et al. Exclusive nitrate to ammonia conversion via boron-doped carbon dots induced surface Lewis acid sites[J]. *Cell Reports Physical Science*, 2022, 3(7): 100961.

[46] XU Y, CHENG C Q, ZHU J W, et al. Sulphur-boosted active hydrogen on copper for enhanced electrocatalytic nitrate-to-ammonia selectivity [J]. *Angewandte Chemie International Edition*, 2024, 63(16): e202400289.

[47] XU B C, CHEN Z X, ZHANG G, et al. On-demand atomic hydrogen provision by exposing electron-rich cobalt sites in an open-framework structure toward superior electrocatalytic nitrate conversion to dinitrogen [J]. *Environmental Science & Technology*, 2022, 56(1): 614-623.

[48] QI R K, WANG Z W, ZHONG M X, et al. Synergistic integration of amorphous cobalt phosphide with a conductive channel for highly efficient electrocatalytic nitrate reduction to ammonia[J]. *Small*, 2023: 2308311.

[49] LUO H X, LI S J, WU Z Y, et al. Relay catalysis of Fe and Co with multi-active sites for specialized division of labor in electrocatalytic nitrate reduction reaction [J]. *Advanced Functional Materials*, 2024: 2403838.

[50] SUN S N, DAI C C, ZHAO P, et al. Spin-related Cu-Co pair to increase electrochemical ammonia generation on high-entropy oxides[J]. *Nature Communications*, 2024, 15: 260.

[51] LIU D X, MENG Z, ZHU Y F, et al. Gram-level NH_3 electrosynthesis via NO_x reduction on a Cu activated Co electrode [J]. *Angewandte Chemie International Edition*, 2024, 63(1): e2315238.

[52] WANG F Z, XIANG J Q, ZHANG G K, et al. Single-atom Co alloyed Ru for electrocatalytic nitrite reduction to ammonia [J]. *Nano Research*, 2024, 17(5): 3660-3666.

[53] HAN S H, LI H J, LI T L, et al. Ultralow overpotential nitrate reduction to ammonia via a three-step relay mechanism [J]. *Nature*

Catalysis, 2023, 6: 402-414.

[54] YANG K, HAN S-H, CHENG C, et al. Unveiling the reaction mechanism of nitrate reduction to ammonia over cobalt-based electrocatalysts [J]. *Journal of the American Chemical Society*, 2024, (2023-12-01) [2024-04-03]. https://doi.org/10.1021/jacs.3c13517.

[55] XIE M S, DAI F F, GUO H X, et al. Improving electrocatalytic nitrogen reduction selectivity and yield by suppressing hydrogen evolution reaction via electronic metal-support interaction [J]. *Advanced Energy Materials*, 2023, 13(21): 2203032.

[56] QIU W X, XIE M H, WANG P F, et al. Size-defined Ru nanoclusters supported by TiO_2 nanotubes enable low-concentration nitrate electroreduction to ammonia with suppressed hydrogen evolution[J]. *Small*, 2023, 19(30): e2300437.

[57] LI P P, JIN Z Y, FANG Z W, et al. A single-site iron catalyst with preoccupied active centers that achieves selective ammonia electrosynthesis from nitrate [J]. *Energy & Environmental Science*, 2021, 14(6): 3522-3531.

[58] MONAI M, JENKINSON K, MELCHERTS A E M, et al. Restructuring of titanium oxide overlayers over nickel nanoparticles during catalysis[J]. *Science*, 2023, 380(6645): 644-651.

[59] PHAN V T T, NGUYEN Q P, WANG B, et al. Oxygen vacancies alter methanol oxidation pathways on NiOOH [J]. *Journal of the American Chemical Society*, 2024, 146(7): 4830-4841.

[60] CHEN W, SHI J Q, WU Y D, et al. Vacancy-induced catalytic mechanism for alcohol electrooxidation on nickel-based electrocatalyst [J]. *Angewandte Chemie International Edition*, 2024, 63(4): e2316449.

[61] PAN F, ZHOU J J, WANG T, et al. Revealing the activity origin of ultrathin nickel metal-organic framework nanosheet catalysts for selective electrochemical nitrate reduction to ammonia: experimental and density functional theory investigations[J]. *Journal of Colloid and Interface Science*, 2023, 638: 26-38.

[62] HU J, HUANG H, YU M, et al. Electron engineering of nickel phosphide for $Ni^{\delta+}$ in electrochemical nitrate reduction to ammonia[J]. *Nano Research*, 2024, (2023-11-04) [2024-01-03]. https://doi.org/10.1007/s12274-024-6470-3.

[63] AJMAL S, KUMAR A, MUSHTAQ M A, et al. Uniting synergistic effect of single-Ni site and electric field of B-bridged-N for boosted electrocatalytic nitrate reduction to ammonia[J]. *Small*, 2024, 2310082.

[64] BU Y G, WANG C, ZHANG W K, et al. Electrical pulse-driven periodic self-repair of Cu-Ni tandem catalyst for efficient ammonia synthesis from nitrate [J]. *Angewandte Chemie International Edition*, 2023, 62(24): e202217337.

[65] ZHOU L M, CHEN X Q, ZHU S J, et al. Two-dimensional Cu plates with steady fluid fields for high-rate nitrate electroreduction to ammonia and efficient Zn-nitrate batteries [J]. *Angewandte Chemie International Edition*, 2024, 63(18): e202401924.

[66] FU Y F, WANG S, WANG Y, et al. Enhancing electrochemical nitrate reduction to ammonia over Cu nanosheets via facet tandem catalysis [J]. *Angewandte Chemie International Edition*, 2023, 62(26): e202303327.

[67] LI P P, LI R, LIU Y T, et al. Pulsed nitrate-to-ammonia electroreduction facilitated by tandem catalysis of nitrite intermediates[J]. *Journal of the American Chemical Society*, 2023, 145(11): 6471-6479.

[68] HUANG K, TANG K, WANG M H, et al. Boosting nitrate to ammonia via the optimization of key intermediate processes by low-coordinated Cu-Cu sites[J]. *Advanced Functional Materials*, 2024: 2315324.

[69] LOU Y Y, ZHENG Q Z, ZHOU S Y, et al. Phase-dependent electrocatalytic nitrate reduction to ammonia on Janus Cu@Ni tandem catalyst [J]. *ACS Catalysis*, 2024, 14(7): 5098-5108.

[70] GU Z X, ZHANG Y C, WEI X L, et al. Intermediates regulation via electron-deficient Cu sites for selective nitrate-to-ammonia electroreduction[J]. *Advanced Materials*, 2023, 35(48): 2303107.

[71] LODAYA K M, TANG B Y, BISBEY R P, et al. An electrochemical approach for designing thermochemical bimetallic nitrate hydrogenation catalysts[J]. *Nature Catalysis*, 2024, 7: 262-272.

[72] ZHANG L H, WU Y Q, ZHU Z Q, et al. Synergistically enhancing nitrate reduction into N_2 in water by N-doped Pd-Cu biochar bimetallic single-atom electrocatalysis[J]. *Biochar*, 2024, 6(1): 8.

[73] XU H, WU J, LUO W, et al. Dendritic cell-inspired designed architectures toward highly efficient electrocatalysts for nitrate reduction reaction[J]. *Small*, 2020, 16(30): e2001775.

[74] XU H, CHEN J L, ZHANG Z H, et al. In situ confinement of ultrasmall metal nanoparticles in short mesochannels for durable electrocatalytic nitrate reduction with high efficiency and selectivity[J]. *Advanced Materials*, 2023, 35(2): 2207522.

[75] HU Q, HUO Q H, QI S, et al. Unconventional synthesis of hierarchically twinned copper as

efficient electrocatalyst for nitrate-ammonia conversion[J]. *Advanced Materials*, 2024, 36(11): 2311375.

[76] WEI J, TANG H, SHENG L, et al. Site-specific metal-support interaction to switch the activity of Ir single atoms for oxygen evolution reaction[J]. *Nature Communications*, 2024, 15(1): 559.

[77] FREY H, BECK A, HUANG X, et al. Dynamic interplay between metal nanoparticles and oxide support under redox conditions[J]. *Science*, 2022, 376(6596): 982-987.

[78] LI Y F, WANG C C, YANG L K, et al. Enhancement of nitrate-to-ammonia on amorphous CeO_x-modified Cu via tuning of active hydrogen supply[J]. *Advanced Energy Materials*, 2024, 14(7): 2303863.

[79] YIN H B, DONG F, WANG Y L, et al. Understanding the activity trends in electrocatalytic nitrate reduction to ammonia on Cu catalysts[J]. *Nano Letters*, 2023, 23(24): 11899-11906.

[80] YANG K W, HAN S H, WANG Y T, et al. Sustainable production and in-place utilization of a liquid nitrogenous fertilizer[J]. *Joule*, 2023, 7(9): 1948-1955.

过渡金属基催化剂电催化硝酸盐还原反应研究进展

罗红霞[1]，陈　俊[2]，杨建平[1*]

1. 东华大学 材料科学与工程学院，纤维材料改性国家重点实验室，上海 201620
2. 澳大利亚伍伦贡大学，澳大利亚创新材料研究所，智能聚合物研究所，ARC 电子材料科学卓越中心，澳大利亚新南威尔士州，伍伦贡 2522

摘　要：大气环境中过量硝酸盐的积累不仅会危害人体健康，还会破坏生态系统的氮循环平衡。在众多硝酸盐去除技术中，电催化硝酸盐还原技术因其环保、操作简便、在可再生能源驱动环境条件下可控等优点而被广泛研究。过渡金属基催化剂由于其储量丰富、成本低、电子结构易调控及电化学活性可观，在电催化领域被广泛应用。此外，过渡金属基催化剂在硝酸盐还原反应动力学、含氮物种适中的吸附能及活性氢供应能力等方面得到广泛研究。基于此，该综述首先讨论了电催化硝酸盐还原机理，分析了两种主要还原产物（N_2 和 NH_3），并从反应机理的角度分析了设计高效硝酸盐催化剂的基本准则。其次，总结了过渡金属 Fe、Co、Ni 及 Cu 四类催化剂在电催化硝酸盐还原方向的研究进展，并提出了其反应活性、反应路径及稳定性的界面调控策略。最后，对电催化硝酸盐还原存在的问题给出了建议，展望了其未来发展机遇。该综述为探索经济有效的过渡金属基催化剂替代高成本贵金属催化剂用于电催化硝酸盐还原反应提供了启示。

关键词：电催化；硝酸盐还原；过渡金属基催化剂；反应机理；氮循环